

Threshold voltage as a measure of molecular level shift in organic thin-film transistors

Cite as: Appl. Phys. Lett. **88**, 043509 (2006); <https://doi.org/10.1063/1.2167395>

Submitted: 19 October 2005 . Accepted: 21 December 2005 . Published Online: 26 January 2006

Oren Tal, Yossi Rosenwaks, Yohai Roichman, Yevgeni Preezant, Nir Tessler, Calvin K. Chan, and Antoine Kahn



View Online



Export Citation

ARTICLES YOU MAY BE INTERESTED IN

[Close look at charge carrier injection in polymer field-effect transistors](#)

Journal of Applied Physics **94**, 6129 (2003); <https://doi.org/10.1063/1.1613369>

[Threshold voltage shift in organic field effect transistors by dipole monolayers on the gate insulator](#)

Journal of Applied Physics **96**, 6431 (2004); <https://doi.org/10.1063/1.1810205>

[An experimental study of contact effects in organic thin film transistors](#)

Journal of Applied Physics **100**, 024509 (2006); <https://doi.org/10.1063/1.2215132>

Lock-in Amplifiers

Zurich Instruments

Watch the Video

Threshold voltage as a measure of molecular level shift in organic thin-film transistors

Oren Tal^{a)} and Yossi Rosenwaks

Department of Physical Electronics, Faculty of Engineering, Tel Aviv University, Tel Aviv 69978, Israel

Yohai Roichman, Yevgeni Preezant, and Nir Tessler

Department of Electrical Engineering, Technion Israel Institute of Technology, Haifa 32000, Israel

Calvin K. Chan and Antoine Kahn

Department of Electrical Engineering, Princeton University, Princeton, New Jersey 08544

(Received 19 October 2005; accepted 21 December 2005; published online 26 January 2006)

The potential across an organic thin-film transistor is measured by Kelvin probe force microscopy and is used to determine directly the pinch-off voltage at different gate voltages. These measurements lead to the determination of a generalized threshold voltage, which corresponds to molecular level shift as a function of the gate voltage. A comparison between measured and calculated threshold voltage reveals a deviation from a simple Gaussian distribution of the transport density of states available for holes. © 2006 American Institute of Physics.

[DOI: 10.1063/1.2167395]

Organic thin-film transistors (OTFTs) present several advantages, such as low-cost processing, mechanical flexibility, and patterning for large-area applications.^{1–5} Improving the performance of OTFTs requires a deep understanding of charge carrier transport mechanisms through the organic layer. One of the key parameters that determine the OTFT performance is the threshold voltage (V_t), defined as the gate-source voltage (V_{GS}) for which there is no space charge region in the organic film.^{6,7} V_t also serves as a reference potential in the determination of charge concentration in organic thin-film transistors. Thus it has a central role in the study of charge related phenomena in organic films⁸ and OTFT optimization.⁹ V_t is conventionally found by extrapolating the drain-source current, measured as a function of V_{GS} , to zero. Recently, we have demonstrated that V_t could be determined without current detection, by finding the gate-screening onset due to charge accumulation in the channel¹⁰ using Kelvin probe force microscopy (KPFM).¹¹ These methods for V_t extraction are based on the detection of the charge accumulation onset in the channel.

In this letter, we present a method for direct determination of the pinch-off voltage (V_{PO}) defined as the drain-source voltage (V_{DS}) for which a zero-charge region is formed at the drain/channel interface, V_t is then extracted from V_{PO} measured for different V_{GS} . These measurements provide essential information on the molecular level position for different gate-source voltages and on the hole density of states in the organic film.

The OTFT structure [Fig. 1(a)] consists of a heavily doped *p*-type silicon gate electrode, a thermally grown 90-nm-thick silicon oxide gate insulator, and 50-nm-thick gold strips evaporated on the oxide to form the source and drain electrodes separated by 13 μm . A thin-film (50 nm) of N,N' -diphenyl- N,N' -bis(1-naphthyl)-1,10-biphenyl-4,4''-diamine (α -NPD) is deposited on the substrate by sublimation from solid source in an ultrahigh vacuum growth chamber and transported under nitrogen atmosphere to a ni-

trogen KPFM glove box (<2 ppm H_2O). KPFM (Autoprobe CP-Veeco Inc. with homemade Kelvin probe electronics) is used for determination of the surface potential profile across the OTFT channel, with a lateral resolution of tens of nanometers. The transistors are scanned for different V_{GS} and V_{DS} applied by a semiconductor parameter analyzer (HP 4155C), which is also used as a monitor for the drain, source,

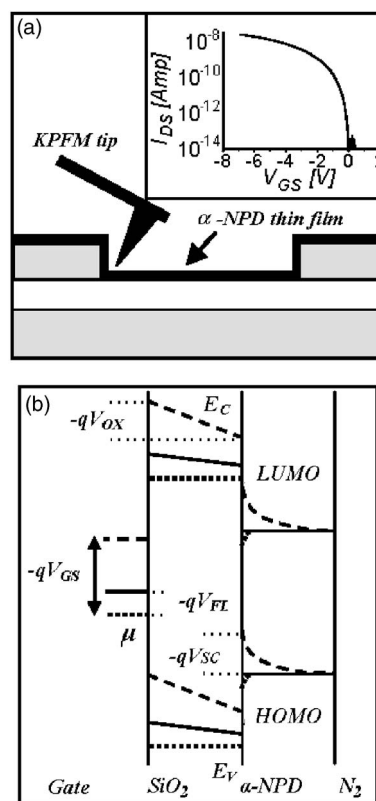


FIG. 1. (a) Schematic of OFET structure and KPFM tip across the channel; (a) Inset I_{DS} - V_{GS} curve measured on the OFET. (b) Schematic energy levels structure across the OFET near the drain for three cases: at equilibrium, $V_{GS}=V_{DS}=0$ V, assuming $V_{FL} \neq 0$ V (dotted curves); at $V_{GS}=V_{FL}$, $V_{DS}=0$ V (solid curves) and at $V_{GS} < V_t$, $V_{DS}=0$ V (dashed curves).

^{a)}Electronic mail: orent@eng.tau.ac.il

and gate currents. The contact resistance,^{9,12} leakage current through the gate-insulator and to the periphery of the active area, and the shift of the threshold voltage⁶ due to continuous voltage application, are found to be negligible in the measured transistors.

The transistor exhibits a *p*-type behavior; i.e., the channel majority carriers are holes, and it is in the “on state” when V_{GS} is lower than V_t . In that state, an accumulation layer is formed near the insulator/semiconductor interface, providing a conducting channel between source and drain. The surface charge concentration induced by the gate for an undoped organic layer is

$$Q = -C_{OX}[V_{GS} - V_t - V(x)], \quad (1)$$

where C_{OX} is the silicon oxide capacitance per unit area, and $V(x)$ is the surface potential at position x across the transistor. $V(x)$ is measured as, $V(x) = CPD(x) - CPD_t(x)$, where $CPD(x)$ is the contact potential difference measured between the KPFM tip and the sample at certain V_{GS} and V_{DS} , and $CPD_t(x)$ is measured at the onset of the conduction channel, at $V_{GS} = V_t$ and $V_{DS} = 0$ V.

V_t can be written as the sum of two contributions:⁶ $V_t = V_{FL} + V_{SC}$, as described by the qualitative energy level scheme across the OTFT channel shown in Fig. 1(b) (possible dipole moments at the interfaces are ignored for simplicity). V_{FL} is the flat level potential that accounts for any work function difference between the organic film and the gate, and for any physical or chemical interface dipole moment or trapped charge at the gate/oxide and oxide/organic interfaces,¹³ and V_{SC} is the voltage drop across the organic semiconductor. V_{SC} is negligible when V_{GS} is in the order of a few volts,⁶ thus as long as V_t equals to a few volts, V_t measured at the onset of the conduction channel can be considered as V_{FL} .

According to Eq. (1) when $V_{DS} = V_{GS} - V_t$, a point with no gate-induced charge is created near the drain, the so-called “pinch-off point.” This takes place at V_{PO} , such that: $V_{PO} \equiv V_{DS} = V_{GS} - V_t$. When $|V_{DS}|$ exceeds $|V_{PO}|$, the pinch-off point shifts towards the source, and a pinch-off region is formed between the drain and the pinch-off point. At any $|V_{DS}|$ larger than $|V_{PO}|$, the potential between the source and the pinch-off point is V_{PO} , and the excess potential $V_{DS} - V_{PO}$ drops across the pinch-off region. Since there is no hole accumulation in this region, its resistance is very high and a small extension of the region is enough to sustain an increase in the potential across it. Consequently, when $|V_{DS}|$ increases, the pinch-off region extends slightly. Our method for extraction of V_t is based on determining V_{PO} by direct observation of the pinch-off phenomenon using a KPFM potential mapping of the channel, and then extracting V_t from V_{PO} .

Figure 2(a) shows potential and topography profiles measured simultaneously across the transistor. The protruding regions on the left and right sides of the bottom topography profile correspond to the source and drain contacts, respectively. The potential profiles were measured for $V_{GS} = -10$ V and V_{DS} ranging between 0 and -10 V. As V_{DS} approaches the pinch-off voltage, a relatively large potential drop appears near the drain (left side). Beyond a certain V_{DS} value, there is almost no change in the potential between adjacent curves, except for a small region near the drain where the abrupt potential drop increases (see the five bottom curves). The large voltage drop across this region is

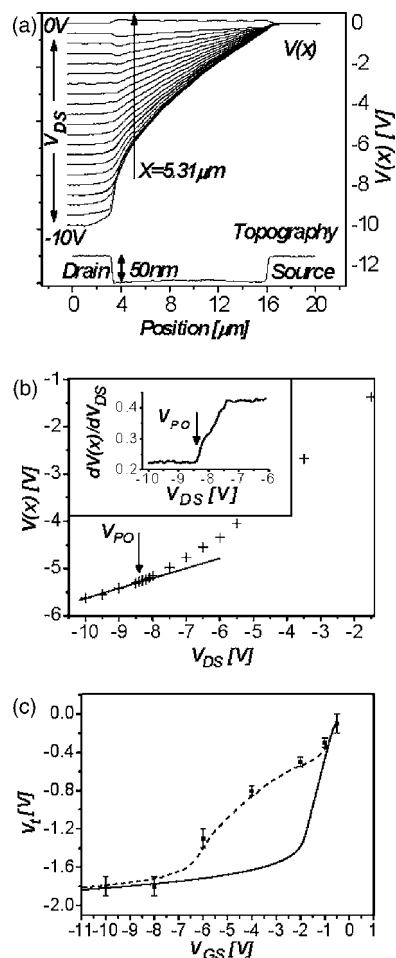


FIG. 2. (a) Topography curve (bottom) and $V(x)$ curves (top) measured by KPFM across the transistor top surface for $V_{GS} = -10$ V and $-10 \text{ V} \leq V_{DS} \leq 0$ V (the upper curve is CPD_t profile). (b) $V(x)$ measured at $1 \mu\text{m}$ to the right of the drain ($x = 5.31 \mu\text{m}$), as a function of V_{DS} and its derivative (inset). The arrows in both cases indicate the V_{PO} value. (c) V_t as a function of V_{GS} —measured (black squares with error bars) and calculated based on a single-Gaussian (full curve) and a two-Gaussians (dashed curve) HOMO-DOS distribution.

ascribed to the abrupt voltage change that is known to occur in the pinch-off region. As long as the (absolute) drain-source bias is smaller than the pinch-off voltage ($|V_{DS}| < |V_{PO}|$), the voltage drop across the accumulation layer increases as the source-drain potential increases. On the other hand, when the drain-source bias exceeds the pinch-off voltage, ($|V_{DS}| > |V_{PO}|$), the potential between the source and the pinch-off point does not change with increasing $|V_{DS}|$, as the excess voltage drop occurs in the pinch-off region in the vicinity of the drain. This is clearly seen in the five bottom curves in Fig. 2(a); however, the curves do not perfectly coincide due to the small shift of the pinch-off point position towards the source as $|V_{DS}|$ increases.

The pinch-off voltage can be accurately determined by plotting the channel potential measured at a specific point, i.e., $1 \mu\text{m}$ to the right of the drain ($x = 5.31 \mu\text{m}$, where x is the lateral position), as a function of increasing V_{DS} as shown in Fig. 2(b). The pinch-off voltage is thus V_{DS} for which $dV(x)/dV_{DS}$ becomes constant [see Fig. 2(b) inset], since any voltage beyond $V_{DS} = V_{PO}$ drops across the pinch-off region. The nonzero derivative is due to the constant lateral shift of the pinch-off point toward the source as V_{DS} increases. We determine V_{PO} at a point x in the channel where the voltage

difference between the curves is maximal, yet far enough from the estimated pinch-off point (\sim maximum curvature point) in order to minimize the tip averaging effect on the measured $V(x)$ (see Ref. 14 for more details about this phenomenon). Based on the pinch-off voltage definition: $V_{PO} \equiv V_{DS} = V_{GS} - V_t$, we can now use V_{PO} extracted at different V_{GS} to determine V_t for different V_{GS} values. Moreover, in the studied case V_{FL} is equal to 0 ± 0.01 V, as determined by the onset of the drain-source current (I_{DS}) [see Fig. 1(a) inset], thus V_t is actually equal to V_{SC} at different V_{GS} . In other words, $-qV_t$ (q denotes the elementary charge) is the shift of the molecular levels at the oxide/organic interface with respect to their equilibrium position as presented in Fig. 1(b).

Figure 2(c) shows a series of V_t extracted in this way for different V_{GS} values (dark squares with error bars). The dependence of V_t on V_{GS} has a direct influence on charge concentration calculations that are based on the threshold voltage [see Eq. (1)]. The dark line in Fig. 2(c) shows calculated V_t as a function of V_{GS} assuming a highest occupied molecular orbital (HOMO) density of states (DOS) with a Gaussian distribution. V_t is extracted from the following model: We use $d^2V/dx^2 = -qp(x)/\epsilon\epsilon_0$ and $p(x) = \int [1 - f(E)] g_i(E) dE$, where V is the potential, p is the hole concentration, ϵ_0 is the dielectric permittivity, $\epsilon = 3$ is the relative dielectric constant of α -NPD,¹⁵ and $f(E)$ is the Fermi-Dirac distribution. In the above expression, $g_i(E)$ is the HOMO Gaussian DOS distribution relevant for holes and given by: $g_i(E) = \{N_i / (\sigma\sqrt{2\pi})\} \exp[-(E/(\sqrt{2}\sigma))^2]$, where $N_i = 1 \times 10^{21}$ cm⁻³ is the total state density, and $\sigma = 0.17$ eV is the Gaussian width (variance). These equations are solved with the following boundary conditions: $(dV/dx)_{x=L} = 0$ and $(V)_{x=0} = V_0$, where V_0 is the potential at the oxide/molecular film interface, and L is the film thickness; V_0 is chosen to satisfy the boundary condition of the electric field being zero at the edge of the molecular layer. Based on the earlier notation, we find: $V_t = (1/2)V_{GAP} - V_0$ and $V_{GS} = V_{OX} + V_t$ where $-qV_{GAP}$ is the energy gap between the HOMO and the lowest unoccupied molecular orbital.¹⁶

The dependence of V_t on the shape of the DOS can be understood by considering that the $-qV_t$ shift is actually the shift of the molecular level with respect to its position in equilibrium at the oxide/organic interfaces near the source. Increasing $|V_{GS}|$ increases the induced hole concentration in the channel, which shifts the chemical potential (μ) towards the center of the DOS. For a Gaussian DOS, the shift is large when the DOS in the distribution tail is low; however, as $|V_{GS}|$ increases, holes accumulate in states of higher density and only small molecular level shifts are required for populating a large number of states. Consequently the calculated V_t shift for a Gaussian DOS is large for small charge concentrations ($|V_{GS}| < 2$ V) and moderate for higher concentrations ($|V_{GS}| > 2$ V). The measured V_t presented in Fig. 2(c) shows a different behavior.

The dashed line in Fig. 2(c) is a calculation of the V_t shift based on a DOS distribution shaped as one main Gaussian ($\sigma = 0.17$ eV, $N_i = 1 \times 10^{21}$ cm⁻³) plus a small secondary Gaussian ($\sigma = 0.1$ eV, $N_i = 1 \times 10^{17}$ cm⁻³) located deeper in the energy gap. The calculated V_t curve based on the two-peak DOS distribution fits the measured V_t very well. This is a strong indication that a realistic DOS edge might deviate considerably from the commonly assumed Gaussian distributions.^{17,18} It is important to emphasize that the calcu-

lated V_t based on the double Gaussian DOS distribution is not a singular solution for a calculated V_t curve that fits to our results, however, this DOS distribution is a simple and yet reasonable one since an additional secondary Gaussian can model an additional DOS distribution due to unintentional doping.¹⁹ Other DOS distributions, different from a simple Gaussian distribution, may also fit the experimental results (i.e., other linear combinations of Gaussian and exponential functions).

In conclusion, we have introduced a method for direct determination of the pinch-off voltage for different gate voltages in organic thin-film transistors using Kelvin probe force microscopy. Based on this method, the threshold voltage was extracted for different gate-source voltages. Changes in this generalized threshold voltage reflect the voltage drop across the organic film perpendicular to the gate electrode, and should be taken into consideration when calculating charge concentrations in organic thin-film transistors. A calculated threshold voltage based on a single Gaussian shaped DOS distribution does not fit the measured threshold voltage, while calculation based on a main Gaussian density of states with an additional secondary Gaussian state distribution located deeper in the energy gap describes the measured data well. This result provides strong evidence, in this particular case, for deviation of the HOMO-DOS edge from the single Gaussian distribution that is commonly used for its description.

This research was supported by the US-Israel Binational Science Foundation (BSF), Grant No. 2000-092. Additional support of the work in Princeton was provided by the NSF (DMR-0408589).

¹C. J. Drury, C. M. J. Mutsaers, C. M. Hart, M. Matters, and D. M. de Leeuw, Appl. Phys. Lett. **73**, 108 (1998).

²S. R. Forrest, IEEE J. Sel. Top. Quantum Electron. **6**, 1072 (2000).

³B. Crone, A. Dodabalapur, Y. Y. Lin, R. W. Filas, Z. Bao, A. LaDuca, R. Sarpeshkar, H. E. Katz, and W. Lin, Nature (London) **403**, 521 (2000).

⁴G. Horowitz, F. Deloffre, F. Garnier, R. Hajlaoui, M. Hmyene, and A. Yassar, Synth. Met. **54**, 435 (1993).

⁵R. H. Friend, IEE Colloq. Mol. Electron. (Digest No. 133), IEE, 2 (1990).

⁶G. Horowitz, R. Hajlaoui, H. Bouchriha, R. Bourguiga, and M. Hajlaoui, Adv. Mater. (Weinheim, Ger.) **10**, 923 (1998).

⁷E. J. Meijer, C. Tanase, P. W. M. Blom, E. van Veenendaal, B. H. Huisman, D. M. de Leeuw, and T. M. Klapwijk, Appl. Phys. Lett. **80**, 3838 (2002).

⁸C. Tanase, E. J. Meijer, P. W. M. Blom, and D. M. de Leeuw, Phys. Rev. Lett. **91**, 216601 (2003).

⁹G. Horowitz, P. Lang, M. Mottaghi, and H. Aubin, Adv. Funct. Mater. **14**, 1069 (2004).

¹⁰O. Tal, Y. Rosenwaks, Y. Roichman, N. Tessler, C. K. Calvin, and A. Kahn, Mater. Res. Soc. Symp. Proc., **145**, 871E (2005).

¹¹M. Nonnenmacher, M. P. O'Boyle, and H. K. Wickramasinghe, Appl. Phys. Lett. **58**, 2921 (1991).

¹²L. Burgi, H. Sirringhaus, and R. H. Friend, Appl. Phys. Lett. **80**, 2913 (2002).

¹³H. Ishii, K. Sugiyama, E. Ito, and K. Seki, Adv. Mater. (Weinheim, Ger.) **11**, 605 (1999).

¹⁴O. Tal, W. Gao, C. K. Chan, A. Kahn, and Y. Rosenwaks, Appl. Phys. Lett. **85**, 4148 (2004).

¹⁵W. Gao and A. Kahn, J. Appl. Phys. **94**, 359 (2003).

¹⁶W. Gao and A. Kahn, J. Phys.: Condens. Matter **15**, S2757 (2003).

¹⁷S. V. Novikov, D. H. Dunlap, V. M. Kenkre, P. E. Parris, and A. V. Vannikov, Phys. Rev. Lett. **81**, 4472 (1998).

¹⁸D. Monroe, Phys. Rev. Lett. **54**, 146 (1985).

¹⁹V. I. Arkhipov, P. Heremans, E. V. Emelianova, G. J. Adriaenssens, and H. Bassler, Appl. Phys. Lett. **82**, 3245 (2003).